A Self-powered wireless bolt for smart critical fastener

Biruk Seyoum, Maurizio Rossi, Davide Brunelli

Department of Industrial Engineering
University of Trento, 38123, Trento, Italy
email: first.last@unitn.it

***Abstract*—In this paper, we present the design of a smart bolt for high-end electro-mechanical systems. The bolt is equipped with temperature sensor, an RF chip and it is powered by a Thermoelectric generator (TEG). The work includes the design choices on the small size TEG, and characterizations of the TEGs and DC-DC converters suitable for ensuring reliability and energy neutral conditions. The characterization was done to determine the amount of power that can be generated from a TEG under different loads and at temperature gradients typical of mechanical environments. Performance demonstrate that the power generated at different temperature gradients extracted by means of a boost converter, is sufficient to guarantee continuous wireless monitoring service for high value critical fastener such as avionic, motorsport, and aerospace.**

Keywords— Smart bolt; TEG; Peltier; IoT; Energy harvesting;

I. Introduction

Guaranteeing the safety and reliability of complex electro-mechanical systems (EMS), which includes different aerial and ground vehicles such as airplanes, space shuttles, automobiles and complex infrastructures such as manufacturing plants, underwater oil & gas pipelines, is the prerequisite of keeping them operational. For this reason, such systems are usually equipped with multitude of sensors whose function is to monitor and report the performance and health of the different parts. Nevertheless, parts of EMS which aren't fitted with sensors which therefore are not monitored and controlled by an automation system in real-time must undergo a periodic manual inspection and maintenance. This manual inspection which has a probability of being either premature or overdue is unreliable and adds extra cost. This is one of the reasons behind the exponential increase in the number of parts of EMS that have started to be actively monitored using different sensors.

Heating and rapid cooling of metals leads to hardening of the metal. This process, although useful to produce different appliances such as hard steel cutting tools, has the downside of making the metal more brittle [1]. In EMS critical fasteners such as bolts that are located close to a large source of heat, such as an engine are subject to this phenomenon. These bolts are also subject to wear and tear caused by over stressing. Over time and due to movement the bolt may also become loose and unable to provide the proper tension to hold the parts together. It is therefore important to monitor the health of critical fasteners in EMS, especially those whose failure leads to a total failure or significant reduction in performance of the whole EMS.

One way of monitoring safety and proper function of critical fasteners in EMS is tracking their temperature. By continuously monitoring the temperature of these fasteners and by using the recorded temperature profile, it would be possible to understand their current state and estimate the duration before the need for a replacement. The tension of the fasteners can also be monitored to have an idea of their loosening. The critical fasteners that are crucial for the proper functioning of the whole system have usually larger diameter and this makes them ideal to fit small temperature sensors and intelligent circuit on the top.

The proposed system is an autonomous temperature sensor module with small form factor that will be installed on top of these fasteners. The module contains a low power microcontroller, a temperature sensor and a RF chip to send the data to a central controller. The module will be powered from a TEG that generates electricity from the temperature gradient of the surface of the critical fastener and the environment. Fig. 1 is a schematic representation of the architecture of the system.

A thermoelectric generator offers a continuous source of energy in places where there is a constant generation of heat such as industrial plants, vehicles and human body [2],[3].

The low efficiency and low power of TEGs [4] had been the major limiting factor in them being utilized in applications that require high power but this trend is changing with the advent of low power electronics [5].

In this work the theory of thermoelectric conversion is summarized along with a brief survey of the state of the art in terms of TEG powered applications. The experimental setup is explained and the obtained results are demonstrated. The power management section describes the results obtained from the characterization of DC-DC converters. Finally, a conclusion is drawn based on the result.

II. Thermo-Electric Conversion

Thermo-electricity is a physical phenomenon where a temperature difference between junctions of two different metals creates an electric potential between the junctions and conversely an electric potential (a flow of current between the junctions) creates a thermal difference between the junctions [6]. A basic thermoelectric circuit is commonly made of two different conductors joined at their free ends and each junction subjected to different temperatures. The voltage at the free end is given by

$$V = \alpha \Delta T \qquad (1)$$

where ΔT refers to the temperature difference between the junctions and α is the difference of the Seebeck coefficient between the two materials. From Fig. 2 the current in the characterization circuit is

$$I = \frac{V}{RL+Rin} \quad (2)$$

where RL is the load resistor, Rin is the TEG's internal resistance value. The power delivered to the load is calculated as

$$P_L = I_L V_L = I_L[\alpha \Delta T - I_L R_{in}] \quad (3)$$

$$P_L = \alpha^2 \Delta T^2 \left(\frac{R_{in}}{(RL+Rin)^2}\right) \quad (4)$$

The maximum power is delivered to the load when RL equals Rin.

$$P_{Lmax} = \frac{\alpha^2 \Delta T^2}{4Rin} \quad (5)$$

If there are N thermocouple modules in a single TEG then the maximum power delivered will be

$$P_{Lmax} = \frac{N^2 \alpha^2 \Delta T^2}{4Rin} \quad (6)$$

The power factor is useful in the evaluation of different kinds of generators. It is defined as the maximum power per unit squared temperature and per unit squared area.

$$\mathrm{PF} = \frac{PLmax}{\Delta T^2 A^2} = \frac{N^2 \alpha^2}{4Rin \Delta A^2} \quad (7)$$

III. RELATED WORKS

The check of the state of the bolts is an issue which several companies are addressing. For example, [7] is a company that produces smart bolts with a built in visual tension indicator. This product measures tension on the bolt and displays the result via a shade of red led mounted on the top of the bolt. Although this is an innovative product, it is not suitable for a coordinated sensing as it would be difficult to interface it into an existing closed loop control system. In [8] General Motors employed smart bolts with a combination of small memory and RFID heads. These bolts are mounted on the engine blocks. As the engine passes through the assembly line, data is read and written to the RFID tag by the machines. This data is used at subsequent stages to verify if correct operation were done at the previous stage of assembly. Here the concern was so much into storing state information during the engine assembly rather than monitoring the health of the bolt itself. To the best of our knowledge we have not come across any other publication or product that monitors different properties of bolts in real time and relays gathered data to a central controller.

Since the very early attempts of using TEGs without intermediate power conditioning for ultralow power applications as in [9][10], there has been a lot of progress in harnessing thermoelectricity for different applications. From the point of view of characterizing a TEG to find the maximum power, [11] proposes an additional numerical analysis to improve the estimation of maximum power by measuring the open circuit voltage and short circuit current. Also [12] presents an interesting idea of finding the thermal resistance of a TEG in a noninvasive way. The design of a patch antenna with a TEG mounted on the top is explored is presented in [13]. This system can be used for different RFID and WSN applications. Whilst, the possibility of powering a network of wireless sensors using a combination of TEGs and DC-DC boosters is explored in [14]. The DC-DC booster efficiency was roughly approximated between 10-50% and the sensor module with an on board Zigbee radio was operating with a 10% duty cycle. In [15] and [16] an interesting application of powering gas sensors in a server farm using heat generated from the servers in the data center is proposed. The experiments include the analysis of performance of a combination of two TEGs as generators and two server boards running benchmark applications as source of thermal energy. The system was functioning with a duty cycle of 0.0027%. Experiments on TEGs, in [3], demonstrated that also wearable sensors can be powered. Depending on the ambient temperature, 0.5 to 5 mW of power was generated and was able to power the autonomous wearable system. An application on [17] demonstrates the use of TEGs to power sensors used in body area networks for assisting healthy aging. The TEGs were powered from body heat. The application scavenges 520 µW of energy at 15° C. The system was able to operate with a 0.4% duty cycle. [18] is also a similar application of harvesting energy from human body heat. On [19] TEGs are used as a power source to monitor deep sea pipelines. The TEG was generating energy from the temperature difference between the pipe and the water. The collected temperature and motion data of the pipe was relayed using optical wireless communication; whilst [20] presents an application for waste heat recovery from a diesel engine. In a different approach [18] presents a model to predict the harvested energy using TEGs and photovoltaics based on factors such as light intensity, temperature gradient, human activity. This model can be adapted to perform theoretical analysis prior to performing any experiment on TEGs.

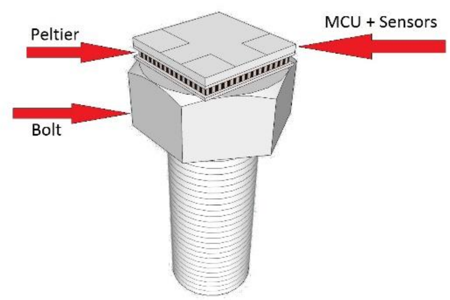

Fig 1. System Model

IV. EXPERIMENTAL SETUP

The design of the self-powered bolt started from the characterization of energy source modules suitable for the EMS application. It was conducted by measuring the output power at different ΔT values at a matched load and at different values of load resistors at a constant gradient. The temperature was measured by NTCLE100E3 thermistors whose R25 = 10 kΩ. The range of the temperature gradient was made as wide as possible to get an idea of the amount of power that can be generated in different scenarios. The acquisition was made using the NI LabVIEW USB-6008 acquisition tool. The module was connected to a LabVIEW project running on a computer, which was sorting and storing the received data. The simple circuit used for the acquisition is as depicted on Fig 2.

When current starts to flow in the circuit the temperature gradient, ΔT, starts to fluctuate due to the Peltier effect [21]. This fluctuation of the temperature gradient also causes a fluctuation of the Seebeck coefficient. Therefore maintaining a constant

Seebeck coefficient is necessary to obtain consistent measurement results. It is therefore compulsory to implement an external circuit to regulate this temperature. In [21] a thermostatting circuit was implemented using two extra TEGs controlled in a feedback loop according to the temperatures of the faces of the main TEG. This has the disadvantage of adding complexity to the simple circuit used for acquisition. Here a different approach was followed instead; and a measurement using direct termostatting regulation was done. Then it was observed that the fluctuation in temperature gradient and the fluctuation of data due to this fluctuation in temperature was negligible, therefore, a simpler approach of applying filter to the data rather than building the complex temperature regulating circuit was chosen. This way the acquisition circuit remained simple.

TABLE 1. SUMMARY OF SPECIFICATIONS OF TEG FROM DATASHEET

Label	TEG specification from datasheet					
	Model	***L [mm]***	***H [mm]***	***Rin [Ω]***	***ΔTmax [K]***	***A*** $[mm^2]$
TEG1	926-1216-ND	26	14	0.25	67	1507
TEG2	926-1192-ND	5	3.4	1.04	67	17
TEG3	926-1225-ND	3.9	3	-	92	15.21

V. EXPERIMENTAL RESULTS

Doing preliminary analytical calculation of the power factor and other parameters according to (4-7) was not possible because of unavailability of important data such as Seebeck coefficient and number of thermocouples from the datasheets. Therefore, only experimental results are reported. The analysis is also based on these experimental results.

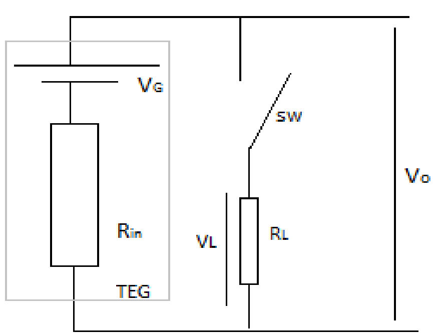

Fig 2. Circuit used for characterization

Table 2 contains the summary of the result of the characterization of TEG 1, TEG 2 and TEG 3. TEG 4 and TEG 5 are **PE127-14-15** and **Thermolife 009r** modules whose result is reported in [21]. TEG 6 is a Peltier module **12706AC** whose result is reported in [22] and finally TEG 7 is a **TEC-12710** whose result is found in [23]. For each module, the power vs load resistance value is measured at 3 different temperature gradient values. The summary of this result is reported in Figures 3, 4 and 5, which are plots of the output power at the load from TEG 1, TEG 2 and TEG 3 respectively. These values were measured for three different temperature gradient values. The measurement was taken by varying the load resistance value between 1 Ω and 10 kΩ. As an example, on Fig. 3 TEG 1 was reported as producing a power of 68 mW at 40° C. Compared to TEG 2 and TEG 3, TEG 1 produces higher output power and this is due to its larger surface. But it can easily be deduced from Table 2 that it has a power factor an order of magnitude lower than the two smaller TEGs.

As the load resistance increases the output power is severely reduced. Peltier modules are usually designed with a low internal resistance to increase the current flow and therefore to absorb more heat when a constant voltage is applied. This is confirmed by the obtained low Rin values and the high current values at matched load.

TABLE 2. SUMMARY OF EXPERIMENTAL RESULTS AND COMPARISONS

Label	Experimental results		
	R_{in} $[\Omega]$	$Pmax/\Delta Tmax$ $[\mu w/K^2]$	**PF** $\mu w/mm^2k^2$
TEG1	1.7	40.625	0.0271
TEG2	2.1	6.94	0.404
TEG3	2.3	6.04	0.397
TEG4	2.23	224	0.14
TEG5	250K	1	0.015
TEG6	1.9	5.31	0.0033
TEG7	1.08	0.25	0.156

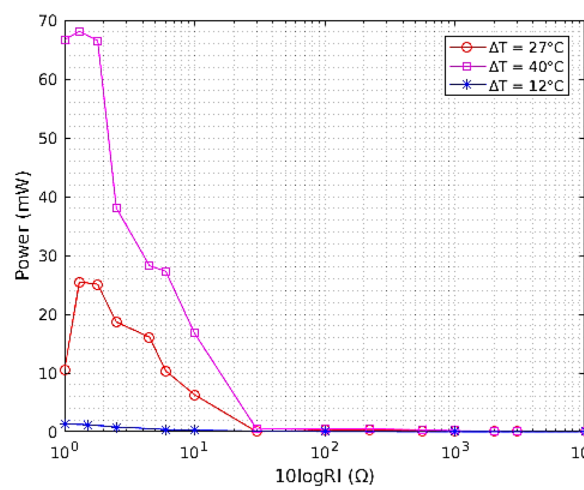

Fig 3. Power vs 10logRL for TEG1

Fig. 6 shows the relationship between the power output per unit area and the temperature gradient at a matched load. Even though TEG 1 generates higher power compared to the other TEGs, due to its larger surface area it has a lower power density compared to the other TEGs.

The open circuit voltage and ΔT also have a linear relationship as stated in (1) and this is depicted on Fig. 7.

VI. POWER MANAGEMENT

Since the voltage from the TEG is very small a boost converter had to be used to step up the voltage. We tested some DC-DC configuration to determine the best efficiency in such extreme conditions.

A. DC-DC Booster Converters

On [21] it was mentioned that TPS60303 was used to boost the generated voltage but this booster has a startup voltage of 0.9V. Since the intention here was using ultra low voltages, the LTC3108 and the Nextreme WPG-1 ultralow voltage step-up converters had been experimented with instead. Among the three modules TEG 3 had the lowest $Pmax/\Delta Tmax^2$ and at 20 degree of ΔT it had an output voltage of 55 mV at a matched load. This is enough to start the LTC3108 and Nextreme WPG-1 converters [24][25].

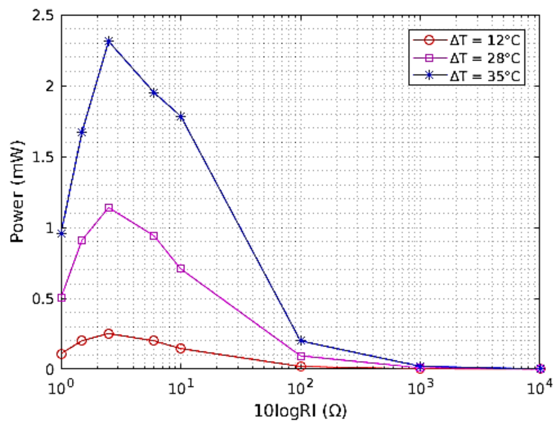

Fig 4. Power vs 10logRL for TEG2

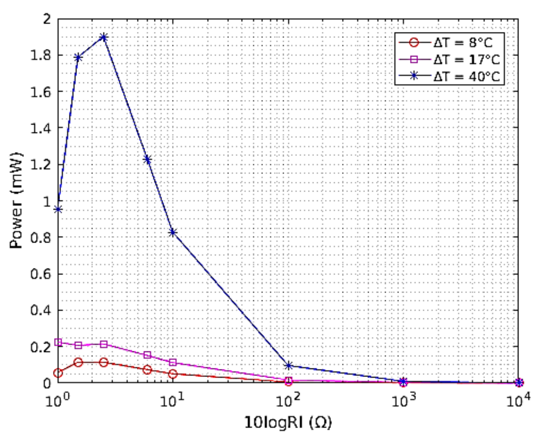

Fig 5. Power vs 10logRL for TEG3

The converters were characterized for their efficiency and charging profile of the output capacitor by supplying them once from the TEG and at another time from a direct DC source while recording the input and output power. The test with the DC source was conducted to assess the efficiency of the converters with large input power. A prototype load which replicated the behavior of an MCU with a radio was used for the characterization of the converters. This load was simulating a radio communication with a duty cycle of 0.5% and it was running with a period of 3 s. The load was consuming 42.15 mW in the active mode and 360 µW in low power mode.

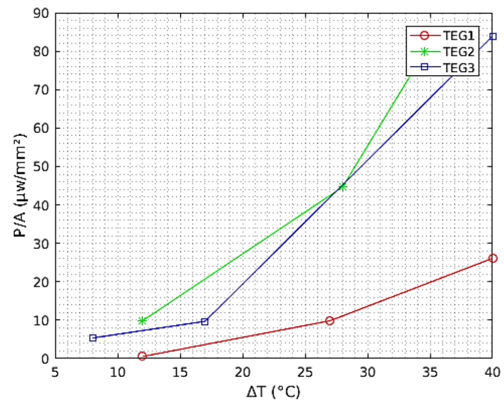

Fig 6. Power vs ΔT at matched load

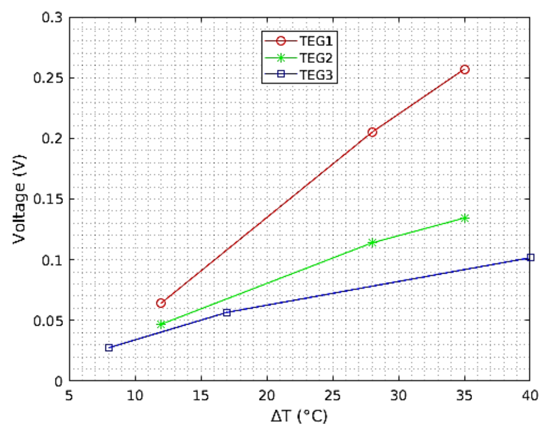

Fig 7. Open circuit voltage Vs ΔT

During the characterization of the dc-dc converters a 22 mF supercapacitor was connected to the output of both boost converters to store charge from the TEG when the load was in low power mode. While performing the experiment the load was connected only after the supercap was charged to 3.3 V. From the charging profile we were able to evaluate the amount of power that gets actually delivered to the supercapacitor and consequently determined the charging time and efficiency of the converters. Due to limited space, only the result for one of these characterizations i.e. the ltc3108 when supplied from the TEG, is shown in Figure 8.

Characterization results for both modules are summarized on Tables 3 and 4. From the result LTC3108 outperformed the Nextreme-WPG1module in both cases. When supplied from the TEG it took the supercap on the Nextreme module about 25 minutes to go above 3V while on the LTC3108 it took close to 40 minutes. Even though the LTC31081 had a higher efficiency (almost a double) it was receiving less input power from the TEG and therefore it took longer time to charge.

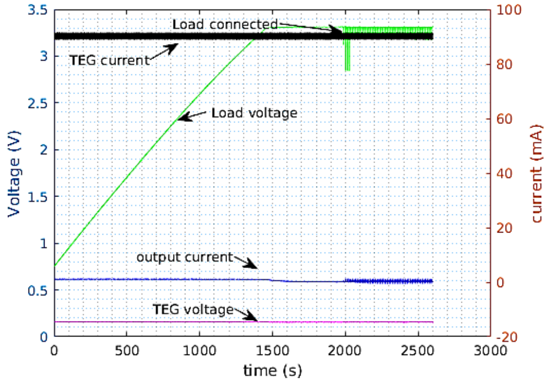

Fig 8. LTC3108 directly supplied from DC

VII. Sensor Application

The smart bolt system consists of two CC1310 low power wireless MCUs from Texas instruments (one as a sender and the other as a receiver) and LTC3108 DC-DC boost converter powered by TEG 2. The CC1310 has an ARM cortex M3 CPU running at 48 MHz with 8 kB of RAM and 128 kB of Flash. The application at the receiver and transmitter was TI-RTOS based.

As reported in Fig. 7 all the modules can start a dc-dc converter from a temperature gradient as low as 15° C. To verify this, TEG 2, with a temperature gradient of 18° C was used as a power source for an autonomous system. Such a difference of temperature between the hot and cold plates of a TEG that is going to be installed on top of a critical fastener is expected in real environments. TEG 2 has a very small area (17mm^2) and it can fit on top of large bolts.

Table 3. LTC3108 characterization result

Supply	LTC 3108 characterization				
	Vin [mV]	*Iout [µA]*	*Pin [mW]*	*Pout [mW]*	*η (%)*
TEG	78	250	1.69	0.83	49.1
DC	477	1000	42	3.16	13.29

The transmitter was supplied by the TEG and it was taking temperature readings from the sensor and transmitting it at 868 MHz in GFSK. The system was tested for its power consumption by varying the packet size and the duty-cycle of the radio. The packet sizes that were tested were 5, 20 and 64 bytes. The transmission were 18ms, 28ms & 76ms respectively. The duty cycle that were tested were [3.6%, 1.8%, 0.6%], [5.6%, 2.8%, 0.9%] & [15.2%, 7.6%, 2.5%] for the 5, 20 & 64byte packets respectively by fixing the interval between transmissions to 500 ms, 1 s and 3 s respectively. Fig. 9 shows the current and voltage of the transmitter with a duty cycle of 3.6%. The packets were transmitted at 14 dBm and they were correctly decoded.

Fig. 10 shows the relationship between duty-cycle and the average power consumption at different packet sizes at the transmitter. As the size of packet increases the current drawn by the MCU, hence the power consumption considerably increases. In fact, the system was not able to sustain itself beyond a packet size of 64 bytes. It is therefore important to put the size of data into consideration while designing energy neutral systems.

Table 4. Nextreme WPG-1 characterization result

Supply	Nextreme WPG-1 characterization				
	Vin [mV]	*Iout [µA]*	*Pin [mW]*	*Pout [mW]*	*η (%)*
TEG	136	380	3.4	0.95	27.1
DC	477	850	43.5	2.6	5.9

Table 5 is a summary of how much power is generated by the TEG at different temperature gradients using the three TEGs and the maximum duty-cycle the system can be sustained with using this power. This system was sinking a 15.3 mA current with a power of 45.75 mW during transmission and 0.39 mA with a power of 1 mW while inactive. The maximum duty-cycle is then calculated using

$$E_{tot} = E_{active} + E_{sleep} \;=\; P_{tx}t_{tx} + P_{sleep}(T - t_{tx}) \quad (8)$$

where E is the energy and T is the total time which is the sum of transmission and sleep times. t_{tx} is already determined from the experiment and is about 200 ms. The efficiency of the DC-DC converter at these temperatures is taken from the characterization of the converters in the previous section and it is used to determine the net power that is delivered to the load. From these results, it is expected to stream temperature data every 2.8 s (7.1% duty-cycle) with a ΔT as low as 10° C employing a TEG 1 as supply of CC1310 MCU through the LTC3801 converter.

Table 5. Estimation of max duty cycle based on input Power

Label	Experimental Result					
	$\Delta T = 10$		$\Delta T = 20$		$\Delta T = 30$	
TEG1	P_{in} (mW)	3.6	P_{in} (mW)	10	P_{in} (mW)	22.5
	$\%d$	7.1	$\%d$	21	$\%d$	48
TEG2	P_{in} (mW)	0.5	P_{in} (mW)	1.3	P_{in} (mW)	1.6
	$\%d$	0.24	$\%d$	2.0	$\%d$	2.6
TEG3	P_{in} (mW)	0.45	P_{in} (mW)	1	P_{in} (mW)	1.4
	$\%d$	0.13	$\%d$	1.3	$\%d$	2.2

VIII. Conclusion

In this work the design of smart bolt for critical fasteners was investigated. Critical fasteners that are crucial for the proper performance of EMS should be monitored using different techniques. Three Peltier modules were characterized to evaluate their performance under different temperature gradients and different loads. Two dc-dc converters we also characterized to determine their efficiency. Finally, a sensor module which was composed of an ARM based RF chip was powered using one of the TEGs and temperature values were transmitted in wireless. Based on the transmission power, the transmit duration, the total power consumption and efficiency data from the characterization of the dc-dc converters, the maximum duty-cycles each TEG could provide to this system under different temperature gradients is analyzed. Starting from these results, we are going to study how to effectively integrate different sensors, in addition to the temperature one, in the top of the smart bolt to extend the set of industrial target applications.

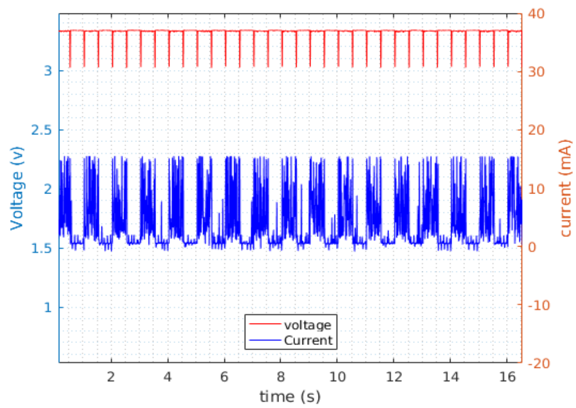

Fig 9 current and voltage at the transmitter

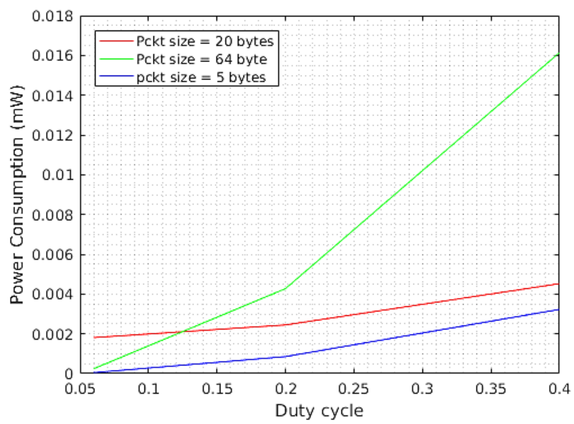

Fig 10 Power consumption Vs duty cycle at different packet sizes

ACKNOWLEDGMENT

Authors would like to thank the IEEE Smart City Initialtive and the Fondazione Cassa di Risparmio di Trento e Rovereto – CARITRO that supported this activity.

REFERENCES

[1] https://depts.washington.edu/matseed/mse_resources/Webpage/Metals/mmetalprocessin.htm
[2] S. E. Jo, M. K. Kim, M. S. Kim and Y. J. Kim, "Flexible thermoelectric generator for human body heat energy harvesting," in Electronics Letters, vol. 48, no. 16, pp. 1013-1015, August 2 2012.
[3] Leonov V, Torfs T, Fiorini P and Van Hoof C 2007 “Thermoelectric converters of human warmth for self-powered wireless sensor nodes” IEEE Sensors J. 7 650-657
[4] G. Pasold, P. Etlin, M. Hahn, U. Muster, V. Nersessian D. Bonfrate, R. Buser, M.Cucinelli, M.Gutsche, M. Kehl, N. Zäch, R. Hazelden “Powering wireless sensors: Microtechnology-based large-area thermoelectric generator for mass applications” sensors, 2011 IEEE.
[5] J. A. Paradiso and T. Starner, "Energy scavenging for mobile and wireless electronics," Ieee Pervasive Computing, vol. 4, pp. 18-27, Jan-Mar 2005.
[6] C. Wu “Analysis of Waste-Heat Thermoelectric Power Generators”. Department of Mechanical Engineering, US Naval Academy, Annapolis, MD. January 1995.
[7] http://www.smartbolts.com/dti/
[8] http://www.popularmechanics.com/cars/a9959/this-bolt-is-the-key-to-gms-high-tech-assembly-line-16324897/
[9] M. A. Sanz-Bobi and R. Palacios, "Potential use of small waste heat sources based on thermoelectricity: Application to an overhead projector and a battery charger", Proc. 5th Eur. Workshop Thermoelectrics, ETS, pp. 58-65, 1999
[10] M. Kishi, H. Nemoto, T. Hamao, M. Yamamoto, S. Sudou, M. Mandai, S. Yamamoto, "Micro thermoelectric modules and their application to wristwatches as an energy source", Proc. 18th ICT, pp. 301-307, 1999
[11] J. Gao and M. Chen, "Beat the Deviations in Estimating Maximum Power of Thermoelectric Modules," in *IEEE Transactions on Instrumentation and Measurement*, vol. 62, no. 10, pp. 2725-2729, Oct. 2013.
[12] F. Attivissimo, A. Di Nisio, C. G. C. Carducci and M. Spadavecchia, "Fast Thermal Characterization of Thermoelectric Modules Using Infrared Camera," in *IEEE Transactions on Instrumentation and Measurement*, vol. 66, no. 2, pp. 305-314, Feb. 2017
[13] M. Virili *et al*., "Design and optimization of an antenna with Thermo-Electric Generator (TEG) for autonomous wireless nodes," *2014 IEEE RFID* Technology and Applications Conference (RFID-TA), Tampere, 2014, pp. 21-25
[14] Madhal, M., Wagnerova, R., Frischer, R. 2011. "Alternative Methods of Power Supply for Autonomous Intelligent Wireless Sensors" 12th International Carpathian Control Conference ICCĆ2011. Velké Karlovice, Czech Republic, 2011, pp. 262-265
[15] Luca Rizzon , Maurizio Rossi , Roberto Passerone , Davide Brunelli, Wireless sensor networks for environmental monitoring powered by microprocessors heat dissipation, Proceedings of the 1st International Workshop on Energy Neutral Sensing Systems, November 13-13, 2013, Rome, Italy
[16] M. Rossi, L. Rizzon, M. Fait, R. Passerone and D. Brunelli, "Energy Neutral Wireless Sensing for Server Farms Monitoring," in IEEE Journal on Emerging and Selected Topics in Circuits and Systems, vol. 4, no. 3, pp. 324-334, Sept. 2014.
[17] D.C. Hoang, Y.K. Tan, H.B. Chng and S.K. Panda "Thernal Energy Harvesting From Human Warmth for Wireless Body Area Network in Medical Health System" PED 2009
[18] D. Fan, L. L. Ruiz, J. Gong and J. Lach, "Profiling, modeling, and predicting energy harvesting for self-powered body sensor platforms," *2016 IEEE 13th International Conference on Wearable and Implantable Body Sensor Networks (BSN)*, San Francisco, CA, 2016, pp. 402-407
[19] S. Amara-Madi, C.A. Price, A. Bensaoula, M. Boukadoum, "Autonomous sensor system for deep-sea pipeline monitoring", *New Circuits and Systems Conference (NEWCAS) 2013 IEEE 11th International IEEE*, pp. 1-4, 2013.
[20] V. Sandu, A. C. Stanca, A. Pasaroiu and D. Dobre, "Experimental investigation of thermoelectric heat recovery from a diesel engine," 2012 International *Conference on Applied and Theoretical Electricity (ICATE)*, Craiova, 2012, pp. 1-8
[21] S. Dalola, M. Ferrari, V. Ferrari, M. Guizzetti, D. Marioli and A. Taroni, "Characterization of Thermoelectric Modules for Powering Autonomous Sensors," in *IEEE Transactions on Instrumentation and Measurement*, vol. 58, no. 1, pp. 99-107, Jan. 2009.
[22] L. Rizzon, M. Rossi, R. Passerone and D. Brunelli, "Energy neutral hybrid cooling system for high performance processors," *International Green Computing Conference*, Dallas, TX, 2014, pp. 1-6.
[23] W. R. Fernandes, Z. Á. Tamus and T. Orosz, "Characterization of peltier cell for the use of waste heat of spas," *2014 55th International Scientific Conference on Power and Electrical Engineering of Riga Technical University (RTUCON)*, Riga, 2014, pp. 43-47.
[24] http://cds.linear.com/docs/en/datasheet/3108fc.pdf
[25] http://www.mouser.com/ds/2/292/Nextreme_Thermobility_WPG-1_Data_Sheet-1931.pdf